Two-dimensional Fe-N-C nanosheets for efficient oxygen reduction reaction

Experimental Section:

Chemical reagent and characterization:

Zinc chloride anhydrous ($ZnCl_2$, >98%) and 2-Methylimidazole (>98%) were obtained from Beijing Innochem Science & Technology co., LTD., Ferric chloride hexahydrate ($FeCl_3 \cdot 6H_2O$, >99%) was purchased Beijing Chemical works. Structure and morphology of prepared catalysts were characterized by scanning electron microscopy (SEM, JSM-7610FPlus, Guangdong, China) with an accelerating voltage of 15 kV. High-resolution transmission (HRTEM) and high angle annular dark-field (HAADF-STEM) (JEM ARM200F, Tokyo, Japan) was performed to explore Fe nanoparticles and atomically dispersed Fe. Powder X-ray diffraction (XRD, Regaku D/Max-2500, Tokyo, Japan) was carried out under Cu Kα radiation at a scanning speed of 5 °/s. X-ray photoelectron spectroscopy (XPS, Scientific EscaLab Xi+, Shanghai, China) was conducted by using an Monochromated Al Ka source under the condition of 1486.6 eV and 15 kV. C 1s at 284.80 eV was used as an internal binding energy standard for correcting charging effects.

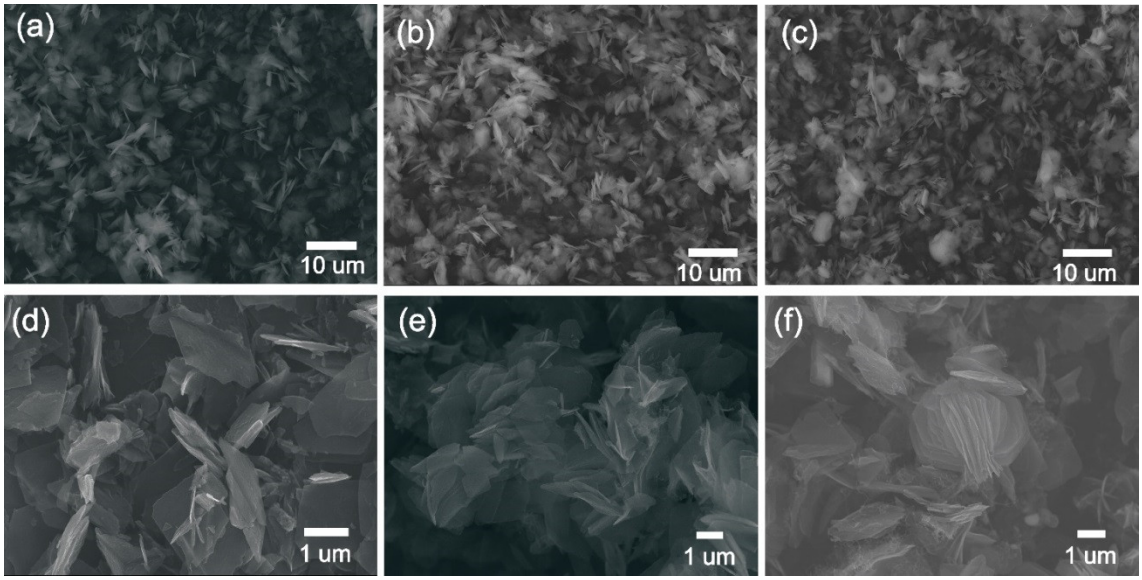

Figure S1. SEM images of Fe/Zn-ZIFs (a–c) and Fe/NCNS (d–f).

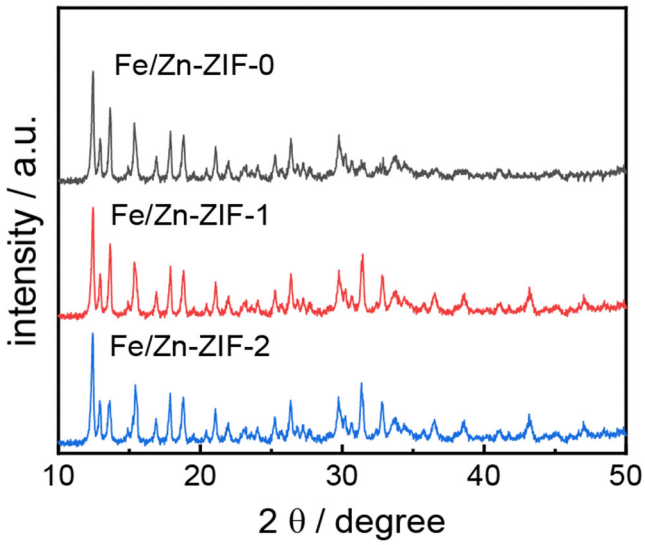

Figure S2. XRD patterns of Fe/Zn-ZIF-0, Fe/Zn-ZIF-1 and Fe/Zn-ZIF-2.

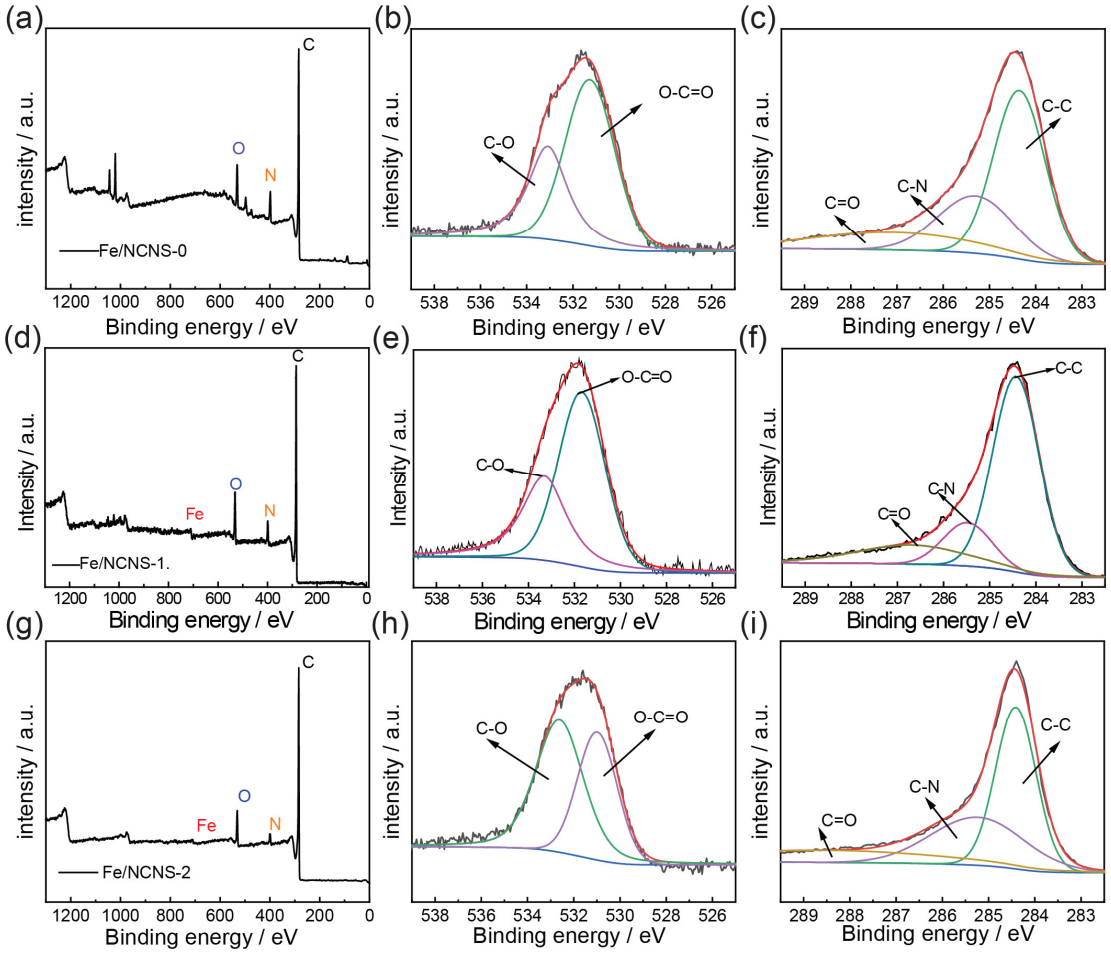

Figure S3. XPS spectra, O 1s spectra and C 1s spectra of Fe/NCNS-0 (a–c), Fe/NCNS-1 (d–f) and Fe/NCNS-2 (g–i).

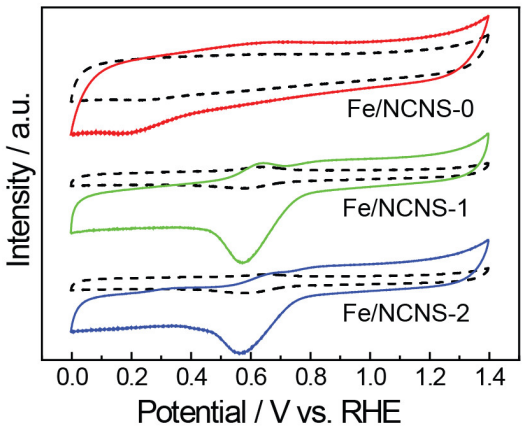

Figure S4. CV curves (scan rate: 50 mV·s^{-1}) in N_2 saturated (black dot line) and O_2 saturated (solid line) 0.5 M H_2SO_4.

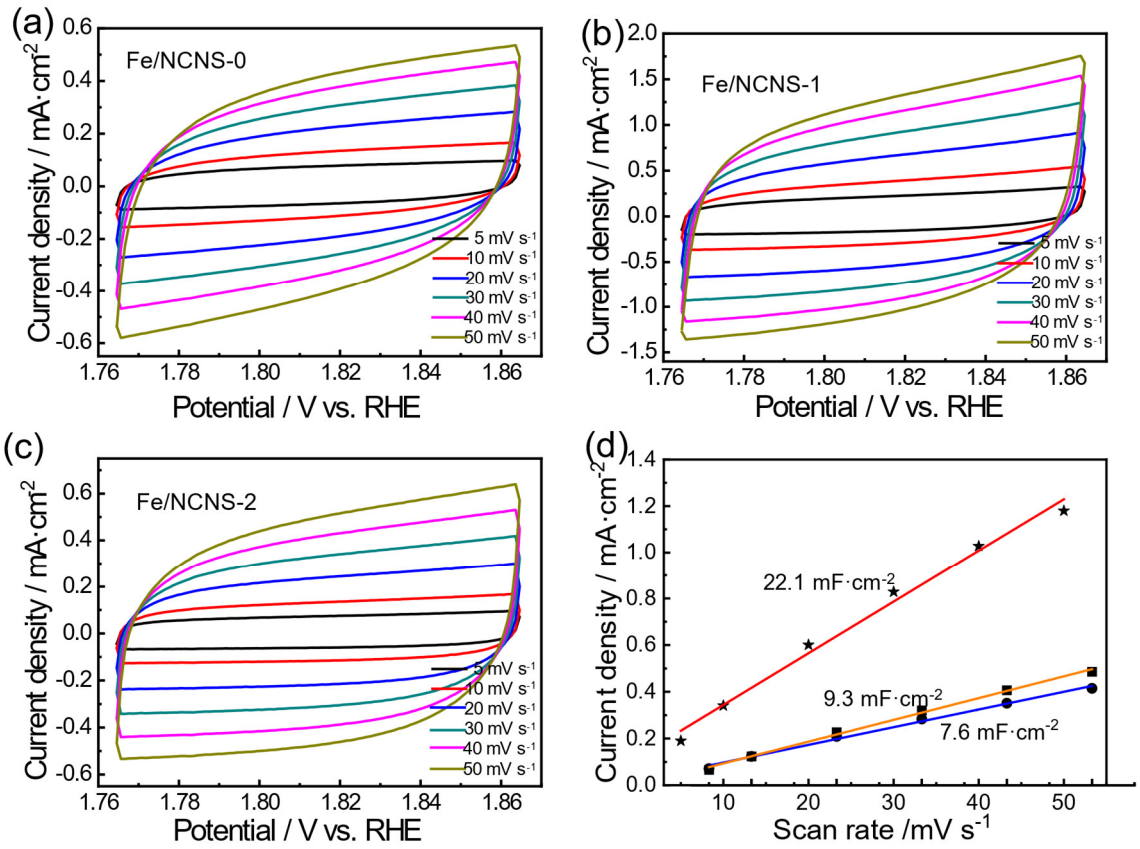

Figure S5. CV curves of Fe/NCNS-0 (a), Fe/NCNS-1 (b) and Fe/NCNS-2 (c) at 5, 10, 20, 30, 40, 50 mV·s^{-1} in 0.5 M H_2SO_4 and corresponding correlation between the current density at 1.81 V and the scan rate (d).

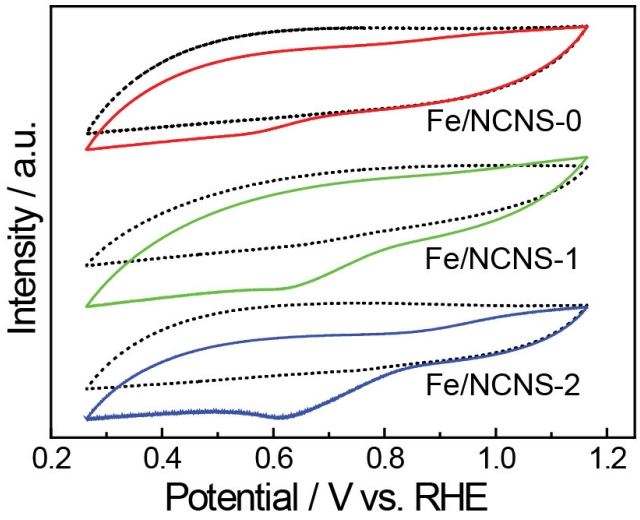

Figure S6. CV curves (scan rate: 50 mV·s^{-1}) in N_2 saturated (black dot line) and O_2 saturated (solid line) 0.1 M KOH.

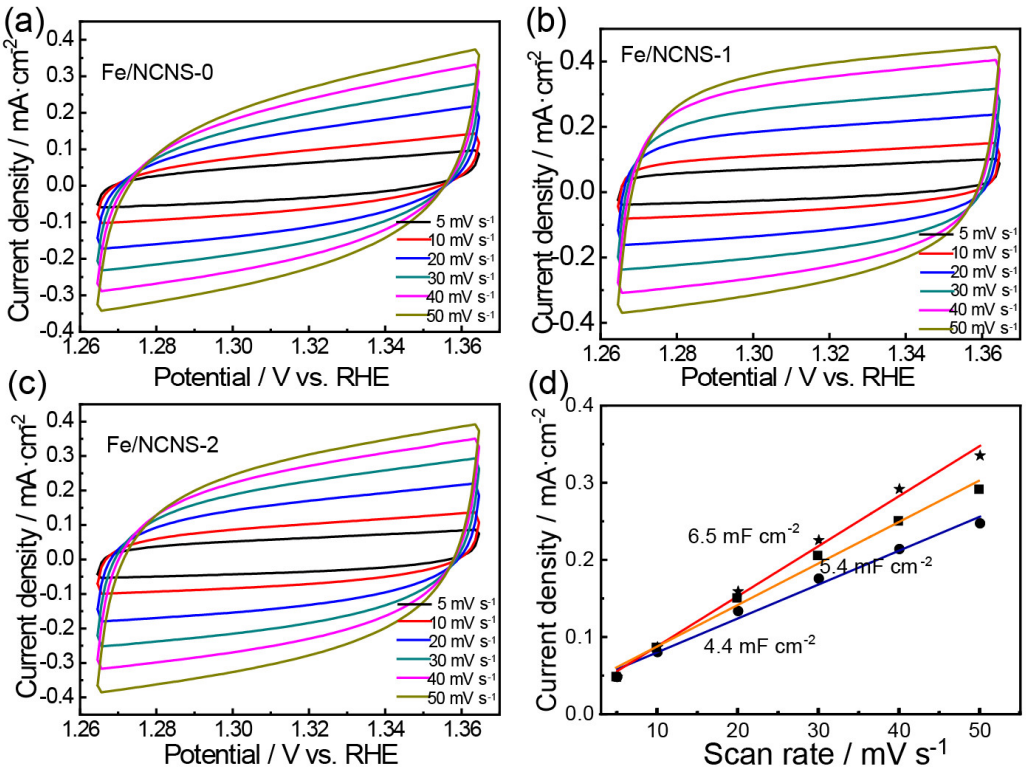

Figure S7. CV curves of Fe/NCNS-0 (a), Fe/NCNS-1 (b) and Fe/NCNS-2 (c) at 5, 10, 20, 30, 40, 50 mV·s^{-1} in 0.1 M KOH and corresponding correlation between the current density at 1.31 V and the scan rate (d).

Table S1 The comparison of ORR activity of Fe/NCNS-1 with reported Fe-based catalysts in acidic electrolyte.

Material	Electrolyte	Half-wave potential	Pt/C	$\Delta(E_{1/2\ Pt/C}-E_{1/2\ material})$	Electron transfer number	Ref.
HP-FeN_4	0.5 M H_2SO_4	0.80 V vs. RHE	N/A	N/A	3.8	[1]
SA-Fe-HPC	0.1 M H_2SO_4	0.81 V vs. RHE	0.84 V vs. RHE	30 mV	4	[2]
FeSAs/PTF-400	0.1 M $HClO_4$	N/A	N/A	N/A	3.99	[3]
FeN_4/HOPC-c-1000	0.5 M H_2SO_4	0.80 V vs. RHE	N/A	20 mV	3.97	[4]
Fe@NMC-1	0.1 M $HClO_4$	0.78 V vs. RHE	0.80 vs. RHE	20 mV	3.86–3.91	[5]
meso-M-N-C/N-G	0.1 M $HClO_4$	0.72 V vs. RHE	0.73 V vs. RHE	10 mV	3.76–3.94	[6]
Co-NOPC	0.5 M H_2SO_4	0.76 V vs. RHE	0.82 V vs. RHE	60 mV	N/A	[7]
Z8-Fe-P	0.1 M $HClO_4$	0.744 V vs. RHE	0.758 V vs. RHE	14 mV	N/A	[8]
C-FeHZ8@g-C_3N_4-950	0.1 M $HClO_4$	0.78 V vs. RHE	0.84 V vs. RHE	60 mV	3.7	[9]
Fe-N-C/HPC-NH_3	0.1 M $HClO_4$	0.803 V vs. RHE	0.846 V vs. RHE	43 mV	3.95	[10]
Fe/NCNS-1	0.5 M H_2SO_4	0.725 V vs. RHE	0.748 V vs. RHE	23 mV	3.98	This work

Table S2 The comparison of Fe-N-C material electrocatalyst with reported in Zn-air baterries.

Materials	Open Circuit Voltage (V)	Power Density ($mW \bullet cm^{-2}$)	Loading Amount ($mg \bullet cm^{-2}$)	Ref.
Fe-TTF-800	1.55	214	2.0	[11]
Fe-SA/NCF	1.45	119	1.2	[12]
5Fe-DPC	1.47	254	1.5	[13]
Fe-1	1.47	201	1.0	[14]
NiFe LDH@Fe-N-CNFs	1.48	157	1.0	[15]
Fe–SA–FPCS	1.51	168	1.5	[16]
Fe_3C–FeN/NC	1.41	166	1.3	[17]
Fe,Ni-N-C/N-CNT	1.46	271	2.0	[18]
Fe/NCNS-1	1.69	1590	5.0	This Work

References

[1] Zhang, N.; Zhou, T.; Chen, M.; Feng, H.; Yuan, R.; Zhong, C. A.; Yan, W.;Tian, Y.; Wu, X.; Chu, W.; Wu, C.; Xie, Y. High-purity pyrrole-type FeN_4 sites as a superior oxygen reduction electrocatalyst. *Energy Environ. Sci*. **2020**, *13*, 111-118

[2] Zhang, Z.; Sun, J.; Wang, F.; Dai, L. Efficient oxygen reduction reaction (ORR) catalysts based on single iron atoms dispersed on a hierarchically structured porous carbon framework. *Angew Chem., Int Ed Engl*. **2018**, *57*, 9038-9043.

[3] Yi, J. D.; Xu, R.; Wu, Q.; Zhang, T.; Zang, K. T.; Luo, J.; Liang, Y. L.; Huang, Y.B.; Cao, R. Atomically dispersed iron–nitrogen active sites within porphyrinic triazine-based frameworks for oxygen reduction reaction in both alkaline and acidic media. *ACS Energy Letters*. **2018**, *3*, 883-889.

[4] Qiao, M.; Wang, Y.; Wang, Q.; Hu, G.; Mamat, X.; Zhang, S.; Wang, S. Hierarchically ordered porous carbon with atomically dispersed fen4 for ultraefficient oxygen reduction reaction in proton-exchange membrane fuel cells. *Angew. Chem. Int. Ed.* **2020**, *59*, 2688-2694.

[5] Chen, X.; Wang, N.; Shen, K.; Xie, Y.; Tan, Y.; Li, Y. Mof-derived isolated fe atoms implanted in N-doped 3d hierarchical carbon as an efficient orr electrocatalyst in both alkaline and acidic media. *ACS Appl. Mater. Interfaces*. **2019**, *11*, 25976-25985.

[6] Huo, L.L.; Liu, B. C.; Zhang, G.; Zhang, J. 2D Layered non-precious metal mesoporous electrocatalysts for enhanced oxygen reduction reaction. *J. Mater. Chem. A*. **2017**, *5*, 4868-4878.

[7] Qiao, M.; Wang, Y.; Mamat, X.; Chen, A.; Zou, G.; Li, L.; Hu, G.; Zhang, S.; Hu, X.; Voiry, D. Rational design of hierarchical, porous, Co-supported, N-doped carbon architectures as

electrocatalyst for oxygen reduction. *ChemSusChem*, **2020**, *13*, 741-748.
[8] Qian, Y.; Liu, Q.; Sarnello, E.; Tang, C.; Chng, M.; Shui, J.; Li, T.; Pennycook, S. J.; Han, M.; Zhao, D. Mof-derived carbon networks with atomically dispersed Fe–N_x sites for oxygen reduction reaction catalysis in acidic media. *ACS Appl. Mater. Interfaces*. **2019**, *1*, 37-43.
[9] Deng, Y.; Chi, B.; Tian, X.; Cui, Z.; Liu, E.; Jia, Q.; Fan, W.; Wang, G.; Dang, D.; Li, M.; Zang, K.; Luo, J.; Hu, Y.; Liao, S.; Sun, X.; Mukerjee, S. g-C_3N_4 promoted mof derived hollow carbon nanopolyhedra doped with high density/fraction of single fe atoms as an ultra-high performance non-precious catalyst towards acidic orr and pem fuel cells. *J. Mater. Chem. A*. **2019**, 5020-5030.
[10] Liu, X.; Liu, H.; Chen, C.; Zou, L.; Li, Y.; Zhang, Q.; Yang, B.; Zou, Z.; Yang, H. Fe_2N nanoparticles boosting FeNx moieties for highly efficient oxygen reduction reaction in Fe-N-C porous catalyst. *J. Nano Research*. **2019**, *12*, 1651-1657.
[11] Zhu, Z.-H.; Yu, B.; Sun, W.; Chen, S.; Wang, Y.; Li, X.; Lv, L.P. Triazine organic framework derived Fe single-atom bifunctional electrocatalyst for high performance zinc air batteries. *J Power Sources*. **2022**, 542.
[12] Wang, W.; Rui, K.; Wu, K.; Wang, Y.; Ke, L.; Wang, X.; Xu, F.; Lu, Y.; Zhu, J. Molecular Bridging Enables Isolated Iron Atoms on Stereoassembled Carbon Framework To Boost Oxygen Reduction for Zinc-Air Batteries. *Chemistry*. **2022**, 2840, e202200789.
[13] Wu, G.; Shao, C.; Cui, B.; Chu, H., Qiu, S.; Zou, Y.; Xu, F.;Sun, L. Honeycomb-like Fe/Fe_3C-doped porous carbon with more Fe–N_x active sites for promoting the electrocatalytic activity of oxygen reduction. *Sustainable Energy & Fuels*. **2021**, 520, 5295-5304.
[14] Sheng, J.; Sun, S.; Jia, G.; Zhu, S; Li, Y. Doping Effect on Mesoporous Carbon-Supported Single-Site Bifunctional Catalyst for Zinc-Air Batteries. *ACS Nano*. **2022**.
[15] Wu, D.; Hu, X.; Yang, Z.; Yang, T.; Wen, J.; Lu, G.; Zhao, Q.; Li, Z.; Jiang, X.; Xu, C. NiFe LDH Anchoring on Fe/N-Doped Carbon Nanofibers as a Bifunctional Electrocatalyst for Rechargeable Zinc–Air Batteries. *Ind Eng Chem Res*. **2022**, 6122, 7523-7528.
[16] Zhu, Y.; Wang, X.; Shi, J.; Gan, L.; Huang, B.; Tao, L.; Wang, S. Neuron-inspired design of hierarchically porous carbon networks embedded with single-iron sites for efficient oxygen reduction. *Sci China Chem*. **2022**, 657, 1445-1452.
[17] Zhou, F.; Yu, P.; Sun, F.; Zhang, G.; Liu, X.; Wang, L. The cooperation of Fe_3C nanoparticles with isolated single iron atoms to boost the oxygen reduction reaction for Zn–air batteries. *J. Mater. Chem. A*. **2021**, 911, 6831-6840.
[18] Fang, J.; Zhang, X.; Wang, X.; Liu, D.; Xue, Y.; Xu, Z.; Zhang, Y.; Song, C.; Zhu, W.; Zhuang, Z. A metal and nitrogen doped carbon composite with both oxygen reduction and evolution active sites for rechargeable zinc–air batteries. *J. Mater. Chem. A.* **2020**, 831, 15752-15759.